

Specsim: The MIRI Medium Resolution Spectrometer Simulator

Nuria P. F. Lorente^{*a}, Alistair C. H. Glasse^a, Gillian S. Wright^a and Macarena García-Marín^b

^aUK Astronomy Technology Centre, Royal Observatory, Blackford Hill, Edinburgh EH9 3HJ, United Kingdom

^bDpto. Astrofísica Molecular e Infrarroja, Instituto de Estructura de la Materia, C/. Serrano 121, 28006 Madrid, Spain

ABSTRACT

MIRI, the Mid-InfraRed Instrument, is one of four instruments being built for the James Webb Space Telescope, and is developed jointly between an European Consortium and the US. In this paper we present a software data simulator for one of MIRI's four instruments: the Integral Field Unit (IFU) Medium Resolution Spectrometer (MIRI-MRS), the first mid-infrared IFU spectrograph, and one of the first IFUs to be used in a space mission. To give the MIRI community a preview of the properties of the MIRI-MRS data products before the telescope is operational, the Specsim tool has been developed to model, in software, the operation of the spectrometer. Specsim generates synthetic data frames approximating those which will be taken by the instrument in orbit. The program models astronomical sources and generates detector frames using the predicted and measured optical properties of the telescope and MIRI. These frames can then be used to illustrate and inform a range of operational activities, including data calibration strategies and the development and testing of the data reduction software for the MIRI-MRS. Specsim will serve as a means of communication between the many consortium members by providing a way to easily illustrate the performance of the spectrometer under different circumstances, tolerances of components and design scenarios.

Keywords: JWST/MIRI, simulations, spectroscopy: integral field, telescopes: jwst, data: modelling, instrument simulation

1. INTRODUCTION

MIRI, the Mid-InfraRed Instrument, is one of four instruments being built for the James Webb Space Telescope (Figure 1), scheduled to be launched in 2013 and placed in a semi-stable orbit at the second Lagrangian point. The design and development of MIRI is being carried out as a collaborative project between an European Consortium of 21 institutes from 10 countries, under the auspices of ESA, and the US. MIRI itself consists of four instruments: an imager, a coronagraph, a low-resolution spectrograph, and an Integral Field Unit (IFU) Medium Resolution Spectrometer (MIRI-MRS). The latter will be the first IFU spectrograph to operate in the mid-infrared, and one of the first such instruments to be used in a space mission.

The MIRI-MRS is an integral field unit (IFU) spectrometer¹, which allows spectroscopy to be carried out on a 2-dimensional area of sky in a single observation. The primary component of the IFU is its image-slicing mirror² (Figure 2), which divides the rectangular field of view into a number of narrow slices. These are then arranged along the entrance slit of a first-order diffraction grating, which carries out the dispersion.

The spectrometer operates in the spectral range 5–28 μm , with a resolution of $R \sim 3000$. The band is divided into 4 IFU channels, which are observed simultaneously. Each channel is equipped with an IFU image slicer designed to match the width of each slice to the diffraction-limited point-spread function of the telescope, at the wavelength of each channel. An observation over the entire spectral band is carried out in a set of three exposures, the spectral band of each IFU channel being subdivided into 3 sub-bands by means of dichroic filters. A diagram showing the relative field of view and spectral bandwidth of each channel and exposure is shown in Figure 3.

* n.lorente@roe.ac.uk; previously N. P. F. M^cKay; www.roe.ac.uk

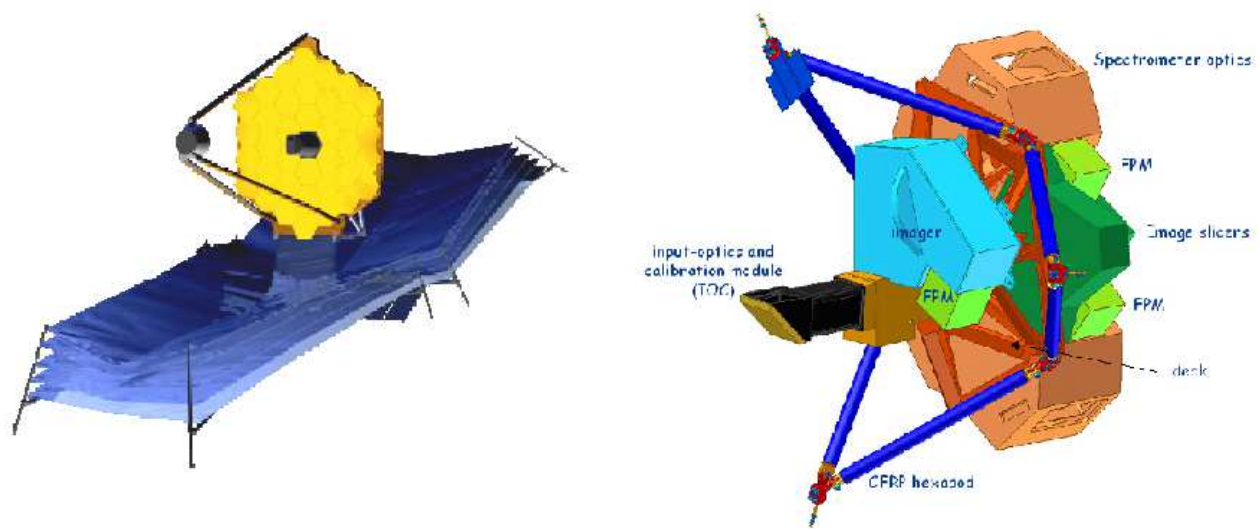


Figure 1. The James Webb Space Telescope (left) and the MIRI instrument (right).

For each of the three exposures, the data are captured on one of two 1024×1024 pixel detectors (one for each pair of image-slicer channels: (1A, 2A), (3A, 4A), (1B, 2B) *etc.*). The expected sensitivity of the instrument is $1.210^{-20} \text{ Wm}^{-2}$ at $6.4 \mu\text{m}$, and $5.610^{-20} \text{ Wm}^{-2}$ at $22.5 \mu\text{m}$, and its spatial field of view widens with increasing channel number, as shown in Figure 3. The main functional parameters for the MIRI-MRS are summarised in Table 1.

The science goals of the MIRI-MRS encompass a broad area of study³, including the formation and evolution of galaxies, the life-cycle of stars and stellar systems, the study of molecular clouds as the focus for star and planet formation, and the investigation of planetary evolution conducive to life.

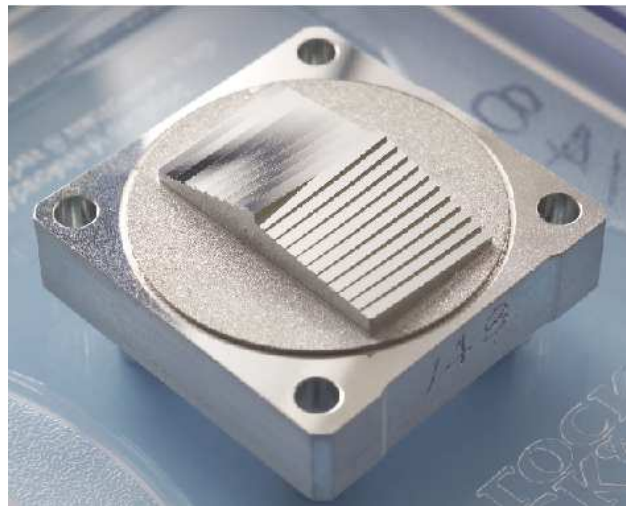


Figure 2. One of the four image slicers for the MIRI Medium Resolution Spectrometer. The slicer shown is for the first spectral channel ($4.87 - 7.76 \mu\text{m}$) which will divide the image plane into 21 slices and align these sub-images with the spectrometer's input slit, in preparation for dispersion. (Photograph credit: Cranfield University, UK).

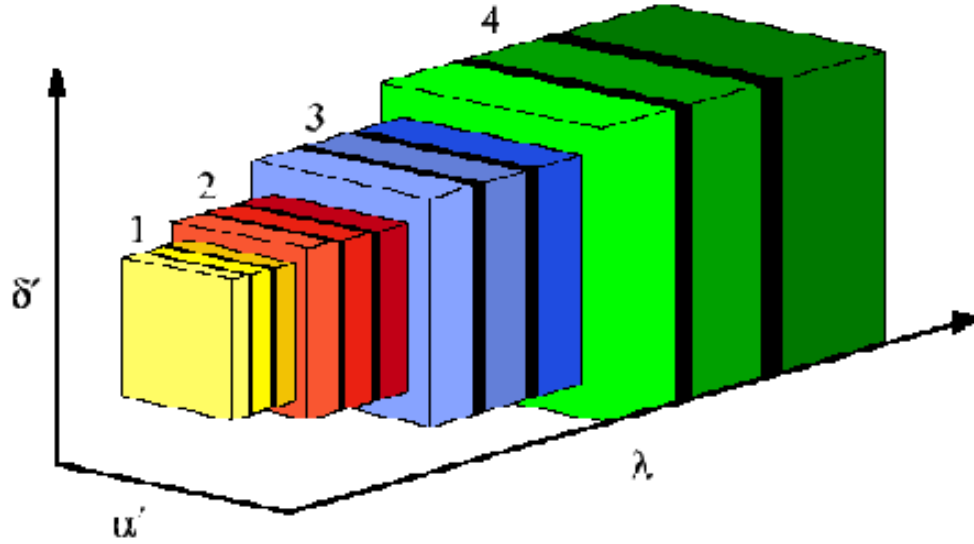
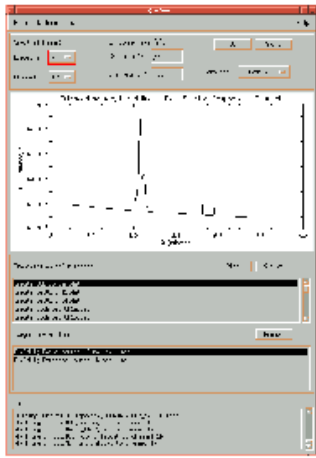


Figure 3. The field-of-view and bandwidth coverage (to scale) of MIRI-MRS channels 1 to 4. The gradation of colour from light to dark in each channel denotes the three exposures A, B and C. The black bands between channels are those spectral regions where the wavelength coverage of adjacent exposures overlap.

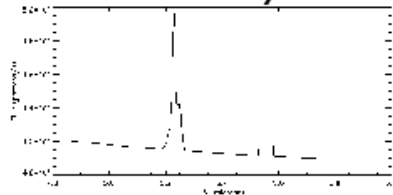
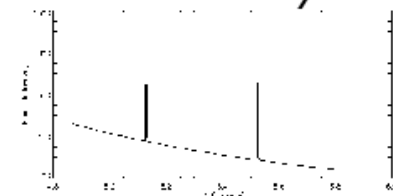
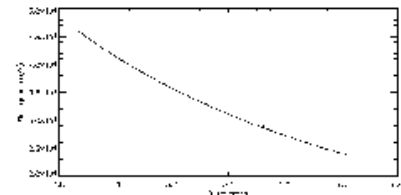
Table 1. Summary of the MIRI-MRS parameters

Channel	FoV (arcsec ²)	Slices	λ (μm)	R_{spectral}	Exposure
1	3.70×3.70	21	4.87 – 5.82	2450 – 3710	A
			5.62 – 6.73		B
			6.49 – 7.76		C
2	4.70×4.51	17	7.45 – 8.90	2480 – 3690	A
			8.61 – 10.28		B
			9.94 – 11.87		C
3	6.20×6.13	16	11.47 – 13.67	2510 – 3730	A
			13.25 – 15.80		B
			15.30 – 18.24		C
4	7.74×7.93	12	17.54 – 21.10	2070 – 2490	A
			20.44 – 24.72		B
			23.84 – 28.82		C

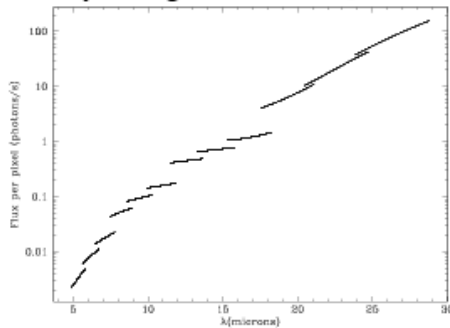
Specsim GUI



Target Models



Sky Background Model



Sky Model

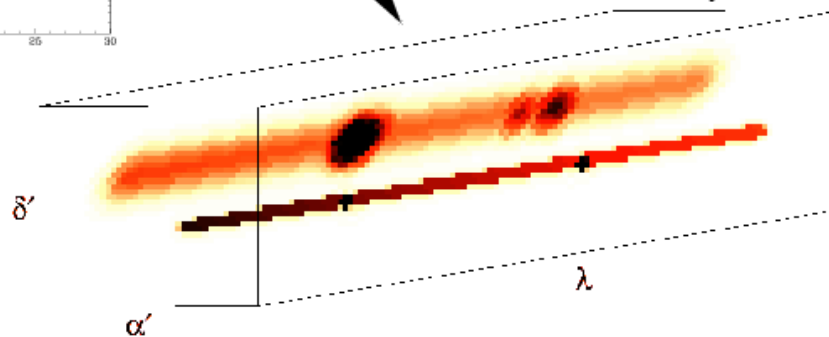


Figure 4. Schematic showing the process of generating the Sky Model (see Section 2.1). The user specifies the required observing parameters (channel, exposure, exposure time, data quality) and loads previously created astronomical target definition files using Specsims's user interface (top-left). When the simulation is started, Specsims creates a model of the field-of-view (the Sky Model, bottom-right) using its internal model of the sky background (centre-left) and the spatial and spectral target definitions imported by the user (top-right). As can be seen in the Sky Model (bottom-left) this particular simulation models a point-source in continuum with two narrow spectral lines, and an extended source with a broad line and two narrow spectral lines.

2. SPECSIM: THE MIRI-MRS SOFTWARE SIMULATOR

Specsim, a software application developed in IDL[†], generates FITS frames which approximate the images which will be produced by the MIRI-MRS. It provides the MIRI community with the opportunity to study the properties of MRS-like data products before the telescope is operational in orbit. Activities such as the design and development of data reduction and analysis software, which require an understanding of the MIRI-MRS data to inform the design process as well as access to datasets with which to test the software tools subsequently developed, can greatly benefit from the availability of simulated data. Similarly, the development of calibration strategies relies on the understanding of the properties of the instrument and their effect on the astronomical data images, and therefore the quality of calibration strategies can be improved if good data models are available.

The process of modelling MIRI-MRS data is carried out by Specsim in two main stages: First, a model of the instrument's field-of-view is created in three dimensions (two spatial and one spectral). This model is then used to generate a detector image, using Specsim's internal model of the JWST and the MIRI-MRS.

2.1. Modelling the Sky

Specsim builds a model of the instrument's field-of-view, for each of the spectrometer's four spectral channels and three exposures. The primary component of this Sky Model is a number of user-defined astronomical target models, generated by means of a set of primitives, provided by the program, with which the user may specify the morphological and spectral characteristics of each target in the field. Currently available target primitives include the following:

Target Morphology:

- Point Source: A point-source, characterised by the point-spread function of the instrument, centred on a user-defined position in (or outside of) the field-of-view.
- Biaxial Gaussian: A Gaussian, with user-specified semi-major and semi-minor FWHM and inclination, and centred on a user-specified position.

Spectral Properties:

- Continuum Properties:

- Black-body Continuum: A simple black-body continuum model, given by

$$F(\lambda) = F_{10} \left(\frac{\lambda_{10}}{\lambda} \right)^5 \frac{e^{\frac{hc}{\lambda_{10}kT}} - 1}{e^{\frac{hc}{\lambda kT}} - 1},$$

with a user-specified $10\mu\text{m}$ flux (F_{10}) and temperature (T).

- Black-body Continuum + Dust: A good approximation of the behaviour of a hot dust component is achieved using a black-body function, modified by λ^{-2} :

$$F(\lambda) = F_{10} \left(\frac{\lambda_{10}}{\lambda} \right)^5 \frac{e^{\frac{hc}{\lambda_{10}kT}} - 1}{e^{\frac{hc}{\lambda kT}} - 1} \times \frac{1}{\lambda^2},$$

with the $10\mu\text{m}$ flux (F_{10}) and temperature (T) specified by the user.

- Polynomial: A continuum model described by the polynomial function

$$F(\lambda) = A + Bx + Cx^2 + Dx^3,$$

where A, B, C and D are given by the user.

- SB99 Model (Young populations): This primitive makes use of the Starburst99 models^{4,5}. The model is well sampled to $\sim 10\mu\text{m}$ (restframe), and is recommended for modelling galaxies at high redshifts. Primitives for starburst models for redshifts $z = 0 - 10$ are available; by default Specsim uses a model corresponding to a young (6 Myr) instantaneous burst of star formation, normalised to a total mass of $10^6 M_{\odot}$, with the Salpeter Initial Mass Function (IMF) and Geneva tracks adapted for a galaxy at a redshift $z = 6$.

[†]IDL is a registered trademark of Research Systems Inc. for their Interactive Data Language software.

- SB99 Model (Intermediate populations): As for the previous continuum type, this primitive makes use of the Starburst99 models^{4,5}. Starburst models at integer redshifts in the range $z = 0 - 10$ may be selected, with the default model corresponding to a 50 Myr old instantaneous burst of star formation, normalised to a total mass of $10^6 M_{\odot}$, with Salpeter IMF and Geneva tracks adapted for a galaxy at redshift $z = 6$.
- Bruzual & Charlot (Old populations): This makes use of the models by Bruzual & Charlot⁶. The model is well sampled to $10 \mu m$ (restframe). The default model corresponds to 2 Gyr old instantaneous burst of star formation, normalised to a total mass of $10^6 M_{\odot}$ with Salpeter IMF and Padova tracks adapted for a galaxy at redshift $z = 6$. As above, starburst models at redshifts in the range $z = 0 - 10$ may also be selected.
- Continuum & PaH Model: This model, developed by Lagache et al.⁷, is valid in the wavelength range $\lambda = 4 \mu m - 3 \text{ mm}$. The default model used by SpecsIm corresponds to an ULIRG of luminosity $L = 5 \times 10^{12} L_{\odot}$, located at redshift $z = 6$, but models in for redshifts $z = 1 - 10$ are also available.
- Broad Spectral Features:
 - Gaussian: A spectral feature defined by the Gaussian function, with a user-specified central wavelength, peak flux and FWHM.
 - $9.7 \mu m$ Silicate: This primitive will load a normalised template of the $9.7 \mu m$ silicate feature and scale it to the requested peak flux.
 - $18 \mu m$ Silicate: This will load a normalised template of the silicate feature at $18 \mu m$ and scale it to the required peak flux.
- Narrow Spectral Lines: Unresolved spectral lines, in emission or absorption, may be defined by specifying the required central wavelength of the line and the line strength. SpecsIm will then use its internal instrument data tables to calculate the appropriate line width, depending on the requested wavelength.

The above primitives may be used individually or in combination, to construct target fields of arbitrary complexity. The target definitions are imported into SpecsIm at run-time, by means of a previously created text file, and together with SpecsIm’s internal models of the zodiacal background, contributions from the telescope’s solar shield, *etc.*, are used to generate a target simulation cube, representing the instrument’s field of view over each channel’s spectral range. This process is illustrated in Figure 4.

2.2. Modelling the MIRI-MRS

Once a model of the target field of view has been produced, SpecsIm simulates the function of the spectrograph, producing a simulated spectroscopic observation of the field. Figure 5 shows a schematic of this process.

The MIRI-MRS model is generated in several stages. First, the contribution to the observed flux by the instrument’s optics and electronics is applied to the sky model. The behaviour of the instrument’s components is described by means of transmission functions, consisting of ASCII files listing the normalised transmission of the subsystem (the efficiency of the mirrors, the behaviour of the detectors, the performance of the dichroics, *etc.*) at each wavelength across the band. The values for the transmission functions may be derived from models of the behaviour of the components or be actual measurements taken during laboratory testing of the individual subsystems. The standard transmission functions are normally loaded automatically by the program. In SpecsIm’s expert mode, however, the transmission functions may be provided by the user, affording extra flexibility in modelling specific aspects of the instrument, simulating faults, and allowing the effect of specific instrument characteristics on the final spectrometer image to be closely studied.

The next step in the process is to simulate the effect of the image slicer, which is done by assigning each pixel in the sky model to an IFU slice, depending on its location in the field of view. Geometric deformations are then applied, simulating the optical path of the telescope, the spectrometer’s pre-optics and the image-slicing mirror.

Dispersion of the image slices is then carried out, by mapping each pixel in the Sky Model onto the corresponding pixel in the detector image, depending on wavelength.

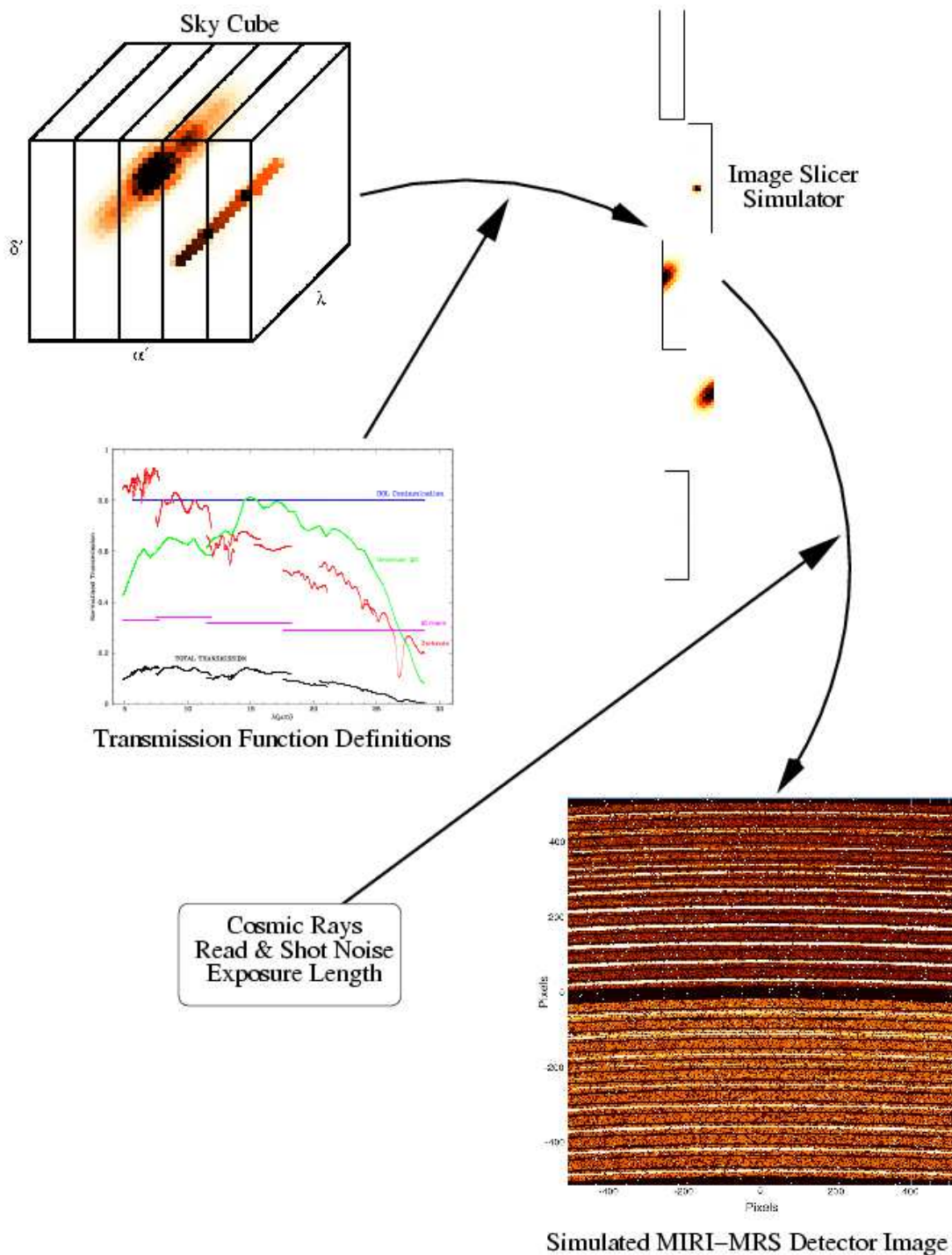


Figure 5. Schematic of the process of generating a simulated detector frame from the Sky Model. The standard or user-provided transmission functions describing the instrument components are loaded and applied to the Sky Model data (centre-left and top-left). The Sky Model is sliced in the spatial dimensions, with the number of slices depending on the spectrometer channel being modelled, and the slices are aligned as for input into the diffraction grating (top-right). Dispersion by the spectrometer is then carried out on the vertically aligned slices, to produce a detector image. Finally, the effects of cosmic rays, integration and noise are implemented on the image, and the simulated spectra for each pair of channels are mapped onto each of two 1024×1024 pixel detectors (bottom-right).

Once the detector image is constructed, on-sky integration is implemented (length of exposure may be supplied by the user) and cosmic rays are added. Cosmic rays have the effect of saturating one or more pixels on the detector, and rendering those pixels invalid for the remainder of the exposure. This results in detector pixels with effective integration times between zero (a cosmic ray hit in the first sub-integration of the exposure) and a full integration (no cosmic ray).

Finally, photon noise and read-noise are added to the detector image, and both the Sky Model and the detector image are provided as FITS files for the user. This allows the detector frames to be processed, analysed and compared with the input targets, thus providing an useful test for the development of the MIRI data reduction software, testing calibration strategies and observation planning.

ACKNOWLEDGMENTS

MIRI draws on the expertise of the following organisations: Ames Research Center, USA; Astron, Netherlands Foundation for Research in Astronomy; CEA Service d’Astrophysique, Saclay, France; Centre Spatial de Liège, Belgium; Consejo Superior de Investigaciones Científicas, Spain; Danish Space Research Institute; Dublin Institute for Advanced Studies, Ireland; EADS Astrium, Ltd., European Space Agency, Netherlands; UK; Institute d’Astrophysique Spatiale, France; Instituto Nacional de Técnica Aeroespacial, Spain; Institute of Astronomy, Zurich, Switzerland; Jet Propulsion Laboratory, USA; Laboratoire d’Astrophysique de Marseille (LAM), France; Lockheed Advanced Technology Center, USA; Max-Planck-Institut für Astronomie (MPIA), Heidelberg, Germany; Observatoire de Paris, France; Observatory of Geneva, Switzerland; Paul Scherrer Institut, Switzerland; Physikalishes Institut, Bern, Switzerland; Raytheon Vision Systems, USA; Rutherford Appleton Laboratory (RAL), UK; Space Telescope Science Institute, USA; Toegepast-Natuurwetenschappelijk Onderzoek (TNO-TPD), Netherlands; UK Astronomy Technology Centre (UK-ATC); University College, London, UK; Univ. of Amsterdam, Netherlands; Univ. of Arizona, USA; Univ. of Cardiff, UK; Univ. of Cologne, Germany; Univ. of Groningen, Netherlands; Univ. of Leicester, UK; Univ. of Leiden, Netherlands; Univ. of Leuven, Belgium; Univ. of Stockholm, Sweden, Utah State Univ. USA.

REFERENCES

1. G. S. Wright, G. H. Rieke, L. Colina, E. van Dishoeck, G. Goodson, T. Greene, P.-O. Lagage, A. Karnik, S. D. Lambros, D. Lemke, M. Meixner, H.-U. Norgaard, G. Oloffson, T. Ray, M. Ressler, C. Waelkens, D. Wright, and A. Zhender, “The JWST MIRI instrument concept,” in *Microwave and Terahertz Photonics*, A. Stohr, D. Jager, and S. Iezekiel, eds., *Proc. SPIE* **5487**, pp. 653–663, 2004.
2. M. Wells, D. Lee, A. Oudenhuysen, P. R. Hastings, J. Pel, and A. C. H. Glasse, “The MIRI Medium Resolution Spectrometer for the James Webb Space Telescope,” in *Astronomical Telescopes and Instrumentation*, *Proc. SPIE*, 2006.
3. Gardener, J. P. et al. *PASP*, 2005. Submitted.
4. C. Leitherer, D. Schaerer, J. D. Goldader, R. M. G. Delgado, C. Robert, D. F. Kune, D. F. de Mello, D. Devost, and T. M. Heckman, “Starburst99: Synthesis Models for Galaxies with Active Star Formation,” *ApJS* **123**, pp. 3–40, 1999.
5. G. A. Vázquez and C. Leitherer, “Optimization of Starburst99 for Intermediate-Age and Old Stellar Populations,” *ApJ* **621**, pp. 695–717, 2005.
6. G. Bruzual and S. Charlot, “Stellar population synthesis at the resolution of 2003,” *MNRAS* **344**, pp. 1000–1028, 2003.
7. G. Lagache, H. Dole, J.-L. Puget, P. G. Pérez-González, E. Le Floch, G. H. Rieke, C. Papovich, E. Egami, A. Alonso-Herrero, C. W. Engelbracht, K. D. Gordon, K. A. Misselt, and J. E. Morrison, “Polycyclic Aromatic Hydrocarbon Contribution to the Infrared Output Energy of the Universe at $z \simeq 2$,” *ApJS* **154**, pp. 112–117, 2004.